JTUSCI

Available online at www.taibahu.edu.sa
ISSN: 1658-3655
Darwish & Alamry / JTUSCI 4: 46-55 (2010)

Journal of Taibah University for Science

Physics

Quasifree pion photoproduction from the deuteron in the energy region from threshold up to the Δ(1232)-resonance including polarization observables

E. M. Darwish[1,2,*] and R. S. Alamry[2]

[1]Physics Department, Faculty of Science, Sohag University, Sohag 82524, Egypt; [2]Applied Physics Department, Faculty of Applied Science, Taibah University, KSA.

Received May 15th 2009; revised October 17th 2010; accepted October 21st 2010

Abstract
Quasifree pion photoproduction from the deuteron including polarization observables is studied in the energy region from threshold up to the Δ(1232)-resonance with inclusion of all leading πNN effects. For the elementary pion photoproduction operator, a realistic effective Lagrangian approach is used which displays chiral symmetry, gauge invariance, and crossing symmetry, as well as a consistent treatment of the spin-3/2 interaction. The interactions in the final two-body subsystems are taken in separable form. The sensitivity of the results to the elementary N(γ,π)N operator is investigated. A considerable dependence on the elementary amplitude of the target asymmetry for the d(γ,π)NN case is found. This indicates that this observable can serve to test different choices of elementary operators .

PACS: 13.60.Le; 25.20.Lj; 25.45.De; 21.45.+v; 24.70.+s; 14.20.-c

Keywords: Deuteron; Meson production; Few-body systems; Photonuclear reactions; Polarization phenomena in reactions; Spin observables.

Corresponding author: eeddarwish@yahoo.com.
Al-Madinah Al-Munawarah, P. O. Box 1343, Kingdom of Saudi Arabia.

1. Introduction

Since the advent of high duty-factor accelerators, such as MAMI at Mainz and ELSA at Bonn (Germany), MAX-Lab at Lund (Sweden), JLab at Newport News and LEGS at Brookhaven (USA), the study of single pion production at intermediate energies has been getting increasing attention [1-15] within the context of hadron structure in the non-perturbative domain of Quantum Chromo-Dynamics (QCD). This is relevant for the study of the nature of the strong interaction and the investigation of the resonance excitations of the nucleon and their photodecay amplitudes. In addition, this reaction serves as a test of our understanding of the chiral pion-nucleon dynamics. A well-known example is the accurate description given by Chiral Perturbation Theory (ChPT) of the very precise data on the S-wave amplitude E_{0+} and the P-wave amplitudes of π^0-photoproduction on the nucleon in the threshold region [16].

Rescattering effects on pion photoproduction from the deuteron were treated approximately by including hadronic rescattering in the final NN- and πN-subsystems [5]. The method of Ref. [5] was applied to the computation of the spin asymmetry with respect to circular photon polarization [6], which determines the Gerasimov-Drell-Hearn (GDH) sum rule [17]. This approach was limited to the Δ(1232)-resonance region because of the employed elementary pion production operator from [2]. This work was improved in Refs. [8,10] (and also in [9] where the model was extended to virtual photons), in which a better elementary production operator from the MAID model [18] was taken, and the role of final-state interaction (FSI) effects on cross sections and polarization observables was studied. More recently, incoherent pion photoproduction on the deuteron has been studied in the Δ(1232)-resonance region [12] using the elementary production operator from the MAID [18] and SAID [19] multipole analyses and including NN-FSI effect. In [14] we have reported on a theoretical prediction for polarization observables of the exclusive π^0 photoproduction from the deuteron in the Δ(1232) resonance region. For the elementary pion photoproduction amplitude, the model of Sato and Lee (SL) [20] was taken.

In this paper we present results for both the charged and neutral pion photoproduction channels of the semi-inclusive reaction $\gamma d \to \pi NN$ in the energy region from threshold up to the Δ(1232)-resonance. Here, in this work, we are extending the work in the preceding papers [5,14]. The extension includes the following important aspects: (i) An enhanced elementary pion photoproduction operator taken from Ref. [21] is used, and (ii) we investigate the sensitivity of the spin-dependent and spin-independent observables to the elementary pion photoproduction operators. The calculation is of theoretical interest because it provides an important test of our understanding of the πNN dynamics, which is a prerequisite for reliable extraction of the pion photoproduction amplitude on the neutron.

This paper is structured as follows: in the next section we briefly outline the electromagnetic and hadronic two-body elementary reactions which we include in our treatment of pion photoproduction on the deuteron. In section 3, a brief review of the framework for the reaction $d(\gamma,\pi)NN$ in which the transition matrix elements are calculated [5] is presented. Results and discussion are presented in section 4, focusing in the sensitivity of our results to the elementary pion photoproduction operator. Throughout the paper we use natural units $\hbar = c = 1$.

2. Elementary Reactions

In this section we will collect the necessary ingredients for the various elementary reactions which govern the process of pion photoproduction from the deuteron. These are the pion photoproduction reaction from free nucleons $\gamma N \to \pi N$, which plays the central part in the reaction, and hadronic two-body scattering reactions, namely NN and πN scattering, which constitute the rescattering effects in the final state.

To study the $\gamma d \to \pi NN$ processes we first need a model for the elementary reaction $\gamma N \to \pi N$. The model we use for this elementary process is the one elaborated in Ref. [21], which has been applied successfully from threshold up to 1 GeV photon energy in the laboratory reference system and succeeds to reconcile [22] pion photoproduction experiments in the Δ(1232) region [23,24] with the latest Lattice QCD calculations of the quadrupole deformation of the Δ(1232) [25]. Recently, the model has also been applied successfully to eta photoproduction from the proton [26].

The model is based upon an effective Lagrangian approach (ELA), which from a theoretical point of view is a very appealing, reliable, and formally well-established approach in the energy region of the mass of the nucleon. The model includes Born terms (diagrams (A)-(D) in Fig. 1), vector-meson exchanges (ρ and ω, diagram (E) in Fig. 1) and all the four star resonances quoted in by the Particle Data Group (PDG) [24] up to 1.7 GeV and up to spin-3/2: Δ(1232), N(1440), N(1520), N(1535), Δ(1620), N(1650), and Δ(1700) (diagrams (F) and (G) in Fig. 1).

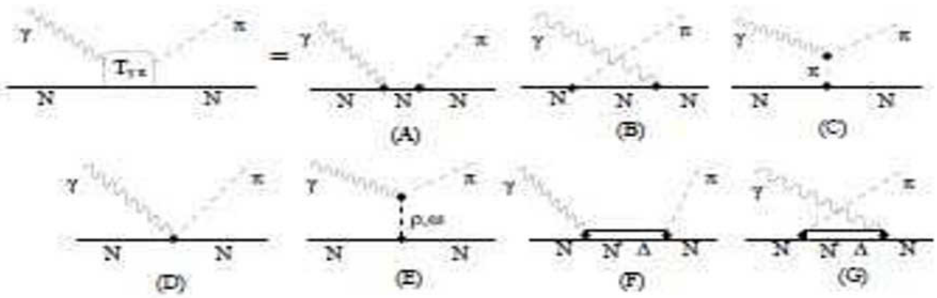

Fig. 1. Feynman diagrams for pion photoproduction from free nucleons. Born terms: (A) direct nucleon pole or s-channel, (B) crossed nucleon pole or u-channel, (C) pion in flight or t-channel, and (D) Kroll-Rudermann contact term; (E) vector meson exchange; resonance excitations: (F) direct or s-channel and (G) crossed or u-channel.

In the pion photoproduction model from free nucleons [21] it was assumed that FSI factorize and can be included through the distortion of the πN final state wave function (pion-nucleon rescattering). πN-FSI was included by adding a phase δ_{FSI} to the electromagnetic multipoles. This phase is set so that the total phase of the multipole matches the total phase of the energy dependent solution of SAID [19]. In this way it was possible to isolate the contribution of the bare diagrams to the physical observables. The parameters of the resonances were extracted by fitting the data to the electromagnetic multipoles from the energy independent solution of SAID [19] applying modern optimization techniques based upon a genetic algorithm combined with gradient based routines [27] which provides reliable values for the parameters of the nucleon resonances. Once the parameters, including phase shifts, are fitted to data we can distinguish between bare and dressed photo-pion production amplitudes on the nucleon. In what follows we call bare amplitudes to the ones provided by our model using the fitted values for all the parameters except those of the phase shifts which are set to zero.

For the interaction in the NN-subsystem we use the separable representations of the realistic Paris potential from [28]. These potentials, called PEST, have become of great use in introducing the features of advanced meson-exchange theory [29] into calculations of few-body systems like nucleon-deuteron scattering [30]. These separable interactions represent a good approximation of the on-shell and off-shell properties of the original Paris potential, providing a good fit to the modern NN database [31]. Thus, the use of such a realistic potential is good enough for our purpose here.

In this work, and for the πN potential in the πN-subsystem, we use the realistic separable representation of πN interaction of Nozawa *et al.* [32]. This model is consistent with the existing unitary description of the πNN system and treats the πN interaction dynamically, with all S-, P- and D-wave πN phase shifts being well reproduced below 500 MeV.

3. Theoretical Treatment of the γd→πNN Reaction

3.1. Kinematics and Cross Section

As a starting point, we will first consider the formalism for quasifree single pion photoproduction from the deuteron

$$\gamma(k,\vec{\varepsilon}_\mu) + d(d) \rightarrow \pi(q) + N_1(p_1) + N_2(p_2)\,, \quad (1)$$

where the four-momenta (k,d,q,p_1,p_2) of the participating particles are indicated within parentheses. The polarization vector of the photon is denoted by $\vec{\varepsilon}_\mu \ (\mu = \pm 1)$. The general formalism for quasifree single pion photoproduction on the deuteron has been described in detail in a previous work [5], and we refer to it for details.

The general expression for the fivefold differential cross section is given by [33]

$$d^5\sigma = \frac{\delta^4(k+d-q-p_1-p_2)\, M_N^2\, d^3q d^3p_1 d^3p_2}{96\,(2\pi)^5\,|\vec{v}_\gamma - \vec{v}_d|\, E_\gamma E_d E_1 E_2 \omega_q} \times \sum_{sm\,\mu m_d} \left| T_{sm\,\mu m_d}(\vec{q},\vec{p}_1,\vec{p}_2,\vec{d},\vec{k}) \right|^2 , \quad (2)$$

where the definition of all kinematical variables and quantum numbers is given in [5]. For the calculation of the cross sections and spin asymmetries we utilize the deuteron rest frame. We have chosen a right-handed coordinate system where the z-axis is defined by the photon momentum $\vec{k}$ and the y-axis by $\vec{k}\times\vec{q}$, where $\vec{q}$ is the pion momentum. The kinematical situation is shown in Fig. 2 in case that the linear photon polarization vanishes. The scattering plane is defined by the momenta of photon $\vec{k}$ and pion $\vec{q}$ whereas the momenta of the two outgoing nucleons $\vec{p}_1$ and $\vec{p}_2$ define the nucleon plane. As independent variables for the characterization of the final state, we choose the outgoing pion momentum $\vec{q} = (q,\theta_\pi,\phi_\pi)$ and the spherical angles $\Omega_p = (\theta_p,\phi_p)$ of the relative momentum $\vec{p} = (\vec{p}_1 - \vec{p}_2)/2 = (p,\Omega_p)$ of the two outgoing nucleons. When the linear photon polarization does not vanish, i.e. $\phi_\pi \neq 0,$ a third plane which spanned by the photon and pion momenta appears. This so-called pion plane makes an angle ϕ_π with the phoon plane.

The semi-inclusive differential cross section, where only the final pion is detected without analyzing its energy, is obtained from (2)

$$\frac{d^2\sigma}{d\Omega_\pi} = \int_0^{q_{max}} dq \int d\Omega_p \frac{\rho_s}{6} \times \sum_{sm\,\mu m_d} \left| T_{sm\,\mu m_d}(\vec{q}, \vec{p}, \vec{k}) \right|^2 , \quad (3)$$

where the maximum pion momentum q_{max} is determined by the kinematics and ρ_s is a phase space factor (see [5] for details).

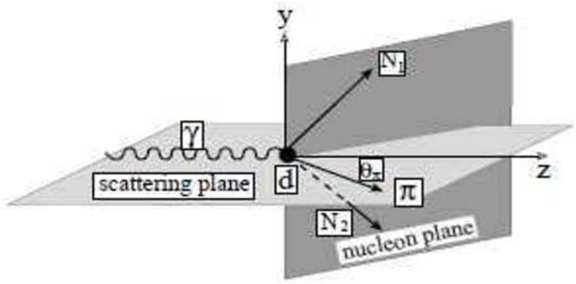

Fig. 2. The kinematics of quasifree pion photoproduction on the deuteron in the laboratory frame in the case when the linear photon polarization vanishes, i.e. $\phi_\pi = 0$.

Regarding polarization observables, we consider in this paper only the linear photon asymmetry Σ and the vector (T_{11}) and tensor(T_{2M}, M=0,1,2) deuteron target asymmetries. The explicit expressions for these asymmetries are given in Refs. [10,12].

3.2. The Photoproduction Amplitude

All observables are determined by the photoproduction amplitude $T_{sm\,\mu m_d}$ of the electromagnetic pion production current $J_{\gamma\pi}$ between the initial deuteron and the final πNN states

$$T_{sm\,\mu m_d}(q, \Omega_\pi, \Omega_p) = -^{(-)}\langle \vec{q}, \vec{p}; sm | \vec{\epsilon}_\mu \cdot \vec{J}_{\gamma\pi}(0) | \vec{d}; 1\, m_d \rangle . \quad (4)$$

In Fig. 3 we show the diagrammatic representation of the scattering matrix. In the calculations, each diagram shown in the figure goes accompanied by the diagram obtained by the exchange $N_1 \leftrightarrow N_2$. In principle, the full treatment of all interaction effects requires a full unitary πNN three-body calculation. In the present work, however, we will restrict ourselves to the inclusion of complete rescattering in the various two-body subsystems of the final state (diagrams (b) and (c) in Fig. 3). Possible two-body contributions to the electromagnetic interaction are neglected. In these respects, the treatment is analogous to previous work [5], to which the reader is referred for formal details. The main difference is that we use a more complete γN→πN amplitude allowing to give a more reliable description of the threshold region and that we include diagram (d) which is not considered explicitly in previous works of Refs. [5,6,8,9,10].

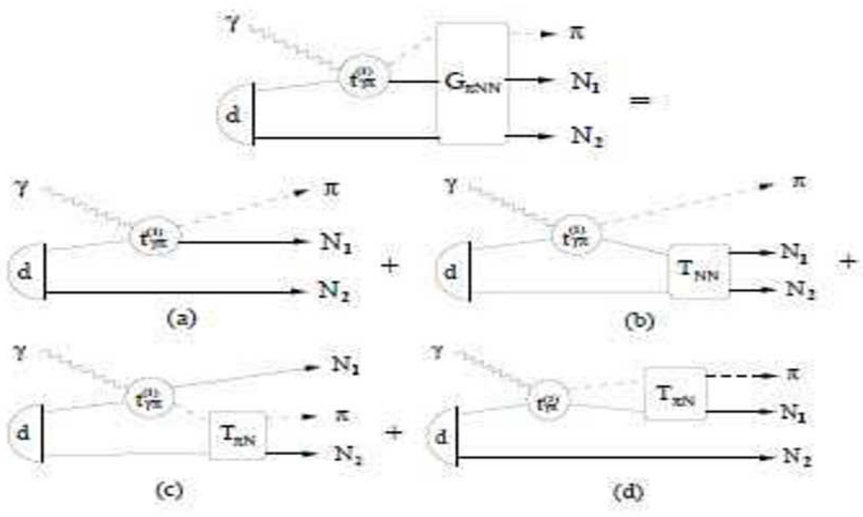

Fig. 3. Diagrammatic representation of the γd→πNN amplitude including rescattering contributions in the two-body subsystems and neglecting all contributions of two-body meson-exchange currents. Diagram (a): impulse approximation (IA); (b), (c), and (d) ``driving terms'' from NN- and πN-rescattering, respectively. In the calculations, each diagram shown in the figure goes accompanied by the diagram obtained by the exchange $N_1 \leftrightarrow N_2$.

For the calculation of the $T_{sm\,\mu m_d}$-matrix we start from the IA (diagram (a) in Fig. 3) to which the contributions from NN- and πN-rescattering (diagrams (b), (c), and (d)) are added. Then, the $T_{sm\,\mu m_d}$-matrix is given by the sum

$$T_{sm\,\mu m_d} = T^{IA_{(a)}}_{sm\,\mu m_d} + T^{NN_{(b)}}_{sm\mu m_d} + T^{\pi N_{(c)+(d)}}_{sm\mu m_d} . \quad (5)$$

For the IA contribution (diagram (a) in Fig. 3), which describes the production on one nucleon while the other acts as a spectator, one has

$$T^{IA_{(a)}}_{sm\,\mu m_d} = \sum_{m'} [\langle sm \,|\langle \vec{p}_1 | t_{\gamma\pi}(W_{\gamma N_1})| - \vec{p}_2\rangle \times \phi_{m'm_d}(\vec{p}_2)|\, 1\, m'\rangle - (1 \leftrightarrow 2)] ,(6)$$

where $t_{\gamma\pi}$ denotes the elementary pion photoproduction operator on the free nucleon; $W_{\gamma N_1}$ is the invariant energy of the γN_1 system, and $\vec{p}_{1/2} = (\vec{k} - \vec{q})/2 \pm \vec{p}$. $\phi_{mm_d}(\vec{p})$ is given by

$$\phi_{mm_d}(\vec{p}) = \sum_{L=0,2} \sum_{m_L} i^L C^{L\,1\,1}_{m_L\, m\, m_d} u_L(p) Y_{Lm_L}(\hat{p}) \quad (7)$$

and we compute the radial deuteron wave function $u_L(p)$ using the realistic Paris potential [34].

The contribution from the NN-rescattering (diagram (b) in Fig. 3) to the transition matrix is

$$T^{NN_{(b)}}_{sm\mu m_d} = \langle \vec{q}, \vec{p}, \, sm \,|\, T_{NN} G_{NN} [t^{(1)}_{\gamma\pi}(W_{\gamma N_1}) + t^{(2)}_{\gamma\pi}(W_{\gamma N_2})] |\, 1\, m_d\rangle , \quad (8)$$

where T_{NN} stands for the half-off-shell matrix of the NN-scattering and G_{NN} for the corresponding free NN propagator. The former is obtained from separable representation of a realistic NN-interaction [28] including all S, P, and D partial waves. Similarly to the NN-rescattering matrix element, we obtain the πN-rescattering contribution (diagrams (c) and (d) in Fig. 3)

$$T^{\pi N_{(c)+(d)}}_{sm\mu m_d} = \sum_{j=c,d} \langle \vec{q}, \vec{p}, \, sm \,|\, T_{\pi N_j} G_{\pi N_j} \times [t^{(1)}_{\gamma\pi}(W_{\gamma N_1}) + t^{(2)}_{\gamma\pi}(W_{\gamma N_2})] |\, 1\, m_d\rangle , \quad (9)$$

where we calculate the half-off-shell πN-scattering matrix $T_{\pi N}$ from a separable energy-dependent πN potential [32] including all S to D waves.

The explicit formal expressions for the three contributions in (6), (8), and (9) can be found in [5] and we refer to this paper for details.

4. Results & Discussion

In this section we compare results for the total cross sections, beam asymmetry, and target asymmetries using different models for the elementary pion photoproduction operator in the energy region from threshold up to the Δ(1232)-resonance for the semi-inclusive $\gamma d \to \pi^0 np$, $\gamma d \to \pi^- pp$, and $\gamma d \to \pi^+ nn$ processes. We obtain an overall good agreement with data where they are available.

We call impulse approximation (IA) to the bare contribution to the observables shown in diagram (a) of Fig. 3 together with the same diagram exchanging $N_1 \leftrightarrow N_2$. In what follows, when we cite any diagram (a)-(d) in Fig. 3 we implicitly mean the contributions of both the depicted diagram and the one obtained by $N_1 \leftrightarrow N_2$ exchange. As stated earlier in [5], the results are rather insensitive to the choice of deuteron wave function.

We would like to explain carefully what we call IA and how we compute it. Our IA calculation (a calculation that includes only diagram (a)) does not employ directly the amplitudes that fit the data on electromagnetic multipoles for the γN→πN process. This is due to the fact that πN-rescattering is unavoidably included in the amplitude in these fits to data. For example, if we use the multipoles provided by the ELA model which fit the experimental data, and afterwards we include πN-rescattering between the pion and the spectator nucleon, we are not really including just diagram (a) + diagram (c), but rather a sort of diagram (a) + diagram (c) + diagram (d), with a contribution of πN-rescattering of the pion with the knocked-out nucleon which comes from the photoproduction operator. For the same reason computations in [5,6,8,9,10] implicitly include to some extent the diagram (d), although it is not explicitly considered, and a certain content of such diagram is also present in the rest of the calculated rescattering terms.

Therefore, if we wish to calculate the contribution coming just from diagram (a), the bare IA contribution to the amplitude has to be extracted from the analysis of the γN→πN, where the final state interaction has to be removed. This was done in Ref. [21]. We name IA* to the calculations where the πN-rescattering is included in the elementary reaction. IA* is, therefore, somehow equivalent to a diagram (a) + diagram (d) calculation. We compare results for IA*+rescattering and IA+rescattering results using the MAID and the dressed ELA models and, thus, we survey the effects of πN-rescattering. We refer to the calculation that includes diagram (b) as NN, to the calculation that includes diagrams (c) and (d) as πN_c and πN_d respectively, and πN to the addition of both πN-rescattering diagrams. Therefore, the full calculation, consistent and with all the effects considered in this work, is what we refer as IA+πN+NN. The calculations performed with the elementary photoproduction operator that implicitly includes diagram (d) will be named as IA*+……..~computations, where the dots stand for NN and πN_c-rescattering, if included. Due to the fact that the dressed ELA and MAID operators include πN-rescattering in the elementary operator, diagram (d) is not included in the calculation of the πN-rescattering when the dressed ELA or MAID multipoles are used.

In this section we explore the dependence of the observables in γd→πNN processes on the input elementary γN→πN reaction. We show results for total cross sections and beam and target asymmetries in the energy region from near threshold to the Δ(1232)-resonance, using as elementary reaction amplitudes the ones provided by the ELA model of Ref. [21] and those obtained using MAID model [18] (Figs. 4, 5, 6, and 7).

The first comparison (Fig. 4) shows total cross sections obtained using bare multipoles from the ELA model (IA+πN+NN, solid), multipoles from the MAID model (IA*+πN_c+NN, dashed), and dressed multipoles from the ELA model (IA*+πN_c+NN, dotted) in all the channels. The total cross section predictions given by the different choices of elementary pion photoproduction operator are similar.

The linear photon Σ asymmetry is defined as $\Sigma = \frac{\sigma_{\parallel} - \sigma_{\perp}}{\sigma_{\parallel} + \sigma_{\perp}}$ where, $\sigma_{\parallel}$ and $\sigma_{\perp}$ stand respectively for the differential cross section for a photon beam with polarization parallel to the scattering plane and the differential cross section for a photon beam with polarization perpendicular to the scattering plane (see Fig. 2). This asymmetry does not exhibit a strong effect of the rescattering contribution and it is an excellent test of any weaknesses in the underlying elementary reaction model. In Fig. 5 we show a sample of our results for Σ.

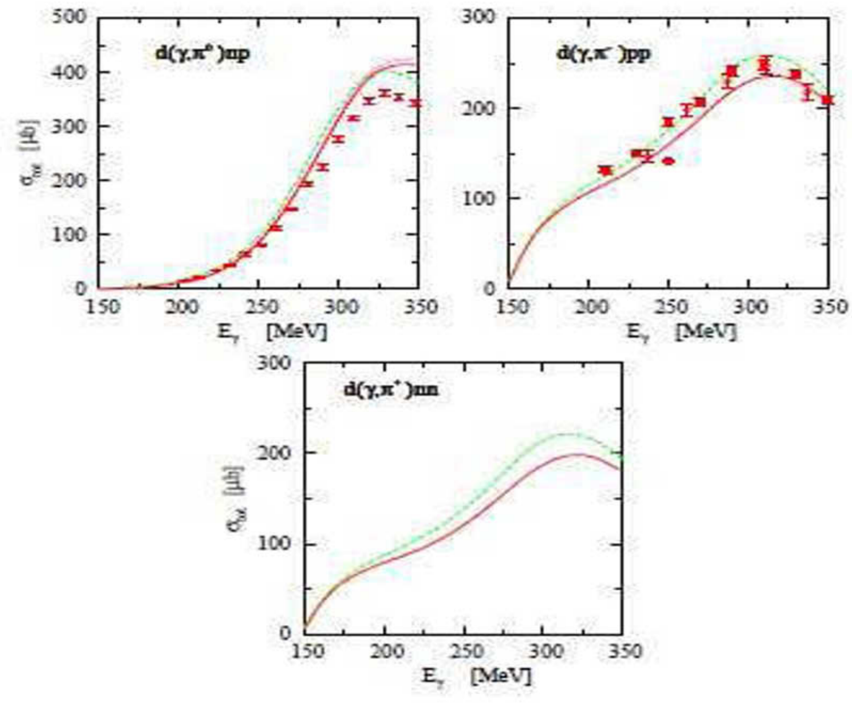

Fig. 4. Total cross section for the separate channels of the reaction d(γ,π)NN using different elementary pion photoproduction operators and including FSI effects. Curve conventions: solid, IA+NN+πN using the bare electromagnetic multipoles of ELA [21]; dashed, IA*+NN+πN_c using MAID [18]; dotted, IA*+NN+πN_c using the dressed multipoles of ELA. IA* denotes the calculation when πN-FSI is included in the elementary reaction (see text). Experimental data from Krusche *et al.* [35] (solid circles) for π^0 channel and from Benz *et al.* [36] (solid squares), Chiefari *et al.* [37] (open circles) and Quraan *et al.* [38] (open squares) for π^- channel.

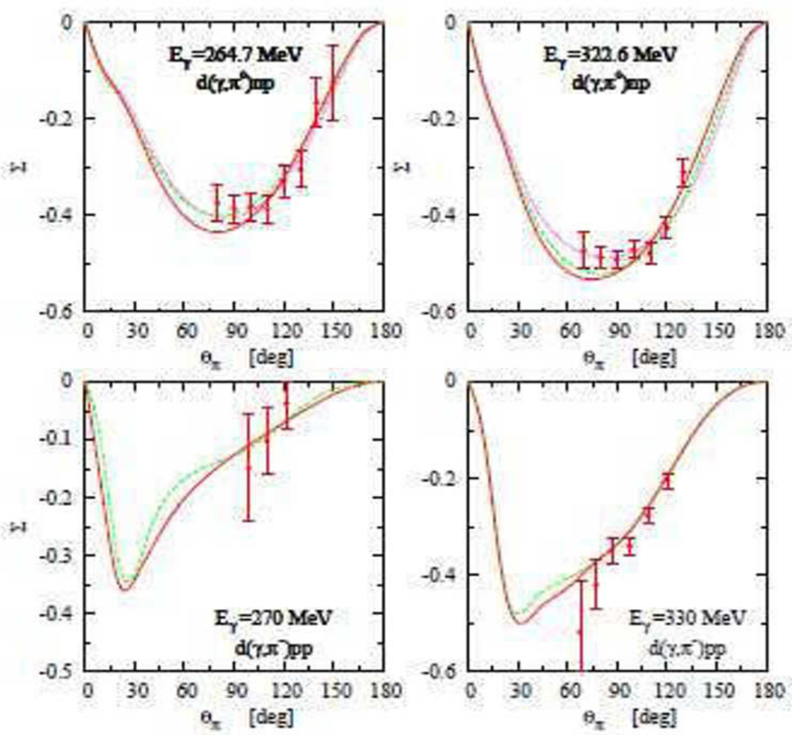

Fig. 5. The beam asymmetry Σ for linearly polarized photons for the $\gamma d\rightarrow\pi^0 np$ (upper two panels) and $\gamma d\rightarrow\pi^- pp$ (lower two panels) processes as a function of pion angle in the laboratory frame of the deuteron at two different photon lab-energies using different elementary pion photoproduction operators and including FSI effects. Curve conventions as in Fig. 4. Experimental data (preliminary) are from the LEGS Collaboration (LEGS-exp-L3b) [39].

If we focus our attention on the target asymmetries in the neutral channel, Fig. 6, similar results are obtained for T_{22}, T_{21}, and T_{20}, but not for the T_{11} asymmetry, where a large difference is found between the computations with the bare multipoles and the dressed ones. In the π^- production channel large differences (qualitative and quantitative) for the T_{11} and the T_{21} asymmetries (Fig. 7) are found when the ELA model (solid line) is compared to the MAID model (dashed line). These differences are due to the photoproduction model and show that the process d(γ,π)NN can be used as a test of the elementary operator employed.

To summarize, the target asymmetries for both neutral and charged channels are found to be very sensitive to the elementary operator. The deviation among results obtained with different operators is very large. It is shown that the process d(γ,π)NN can serve as a test of different elementary operators, since its asymmetry predictions show very different values when one changes the elementary pion production operators employed. Further improvements of the present model (in particular, its extension to higher energies) can be achieved by including the next leading correction from the intermediate NN, NN^*, and NΔ interactions. This may result in an even better agreement between experimental data and theoretical predictions, in particular in the case of π^0 production. It would also be interesting to investigate whether the differences found between the ELA and MAID elementary operators for the predictions of some observables in pion production from deuteron are also seen in pion production from the nucleon.

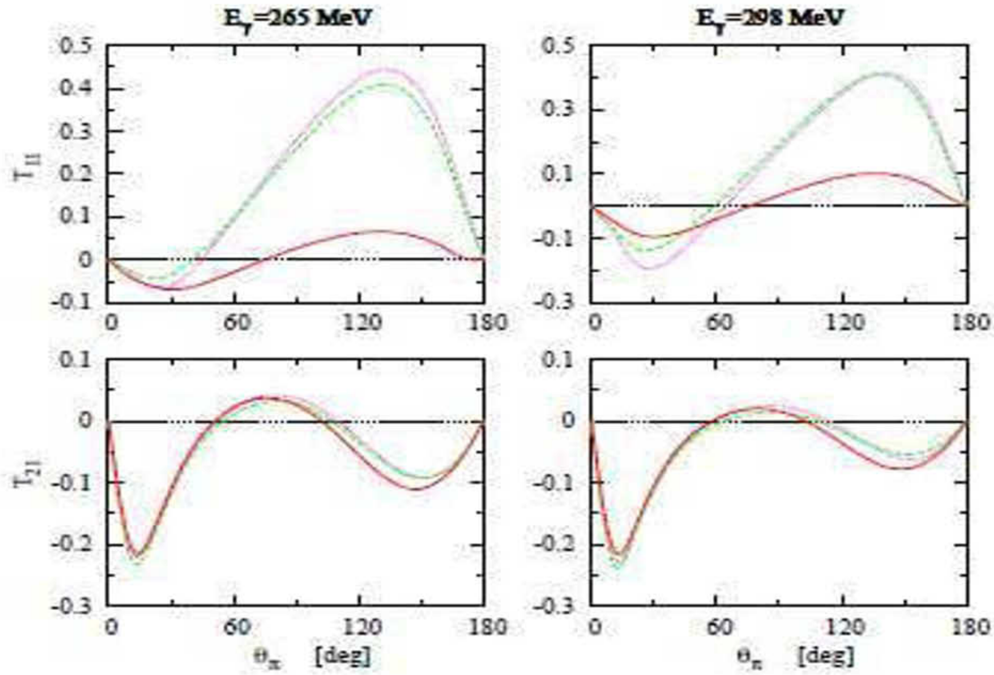

Fig. 6. Single-spin target asymmetries T_{11} and T_{21} for π^0 photoproduction from the deuteron at E_γ=265 and 298 MeV using different elementary pion photoproduction operators and including FSI effects. Curve conventions as in Fig. 4.

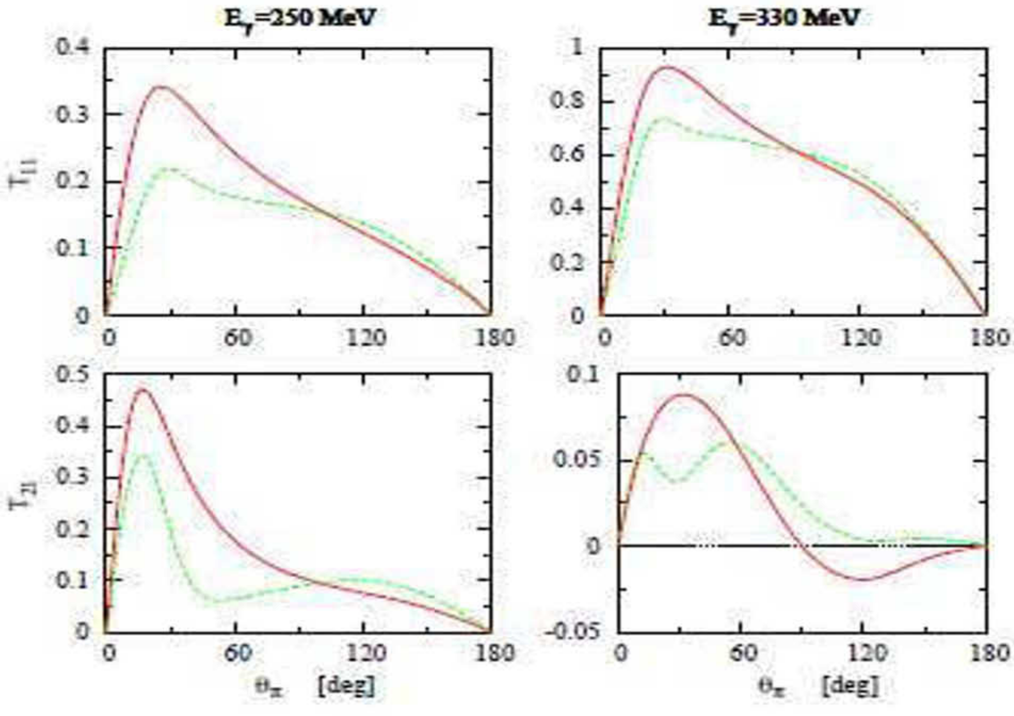

Fig. 7. Same as in Fig. 6 but for π^- production channel at E_γ=250 and 330 MeV. Solid line stands for the full calculation with the ELA model and the dashed line stands for the calculation using MAID model.

Acknowledgements

E. M. Darwish would like to thank C. Fernandez-Ramirez, E. Moya de Guerra, and J. M. Udias for stimulating discussions, a critical and careful reading of the manuscript and A. bdulnaby for keen interest to provide assistance with computing difficulties.

References

[1] H. Garcilazo and E. Moya de Guerra, Phys. Rev. C 49, R601 (1994); H. Garcilazo and E. Moya de Guerra (1995). Phys. Rev. C 52, 49; K.A. Bugaev, U. Oelfke, and P.U. Sauer, arXiv:nucl-th/9811053; A. Loginov, A. Sidorov, and V. Stibunov (2000) Phys. Atom. Nucl. 63, 391 [Yad. Fiz. 63, 459 (2000)]; I.T. Obukhovsky, V.I. Kukulin, M.M. Kaskulov, P. Grabmayr, and A. Faessler (2003) J. Phys. G 29, 2207; K. Kossert et al. (2004) Eur. Phys. J. A 19, 391; H. Krebs, V. Bernard, and U.-G. Meissner (2003). Nucl. Phys. A 713, 405; E.M. Darwish (2004) Nucl. Phys. A 735, 200; E.M. Darwish (2005) J. Phys. G 31, 105; E.M. Darwish and A. Salam (2005) Nucl. Phys. A 759, 170; C. Reiss, H. Arenhoevel, and M. Schwamb (2005). Eur. Phys. J. A 25, 171; PIONS@MAX-Lab Collaboration, K.G. Fissum et al.,http://www.maxlab.lu.se/kfoto/Research_program/np014/np014.html.

[2] R. Schmidt, H. Arenh\"ovel, and P. Wilhelm, Z (1996). Phys. A 355, 421.

[3] J.C. Bergstrom, R. Igarashi, J.M. Vogt, N. Kolb, R.E. Pywell, D.M. Skopik, and E. Korkmaz (1998). Phys. Rev. C 57, 3203.

[4] M.I. Levchuk, M. Schumacher, and F. Wissmann, (2000). Nucl. Phys. A 675, 621.

[5] E.M. Darwish, H. Arenhoevel, and M. Schwamb (2003) Eur. Phys. J. A 6, 111.

[6] E.M. Darwish, H. Arenhoevel, and M. Schwamb, (2003). Eur. Phys. J. A 17, 513.

[7] B. Krusche and S. Schadmand, Prog. Part. Nucl. Phys. 51, 399 (2003); V. Burkert and T.-S.H. Lee, (2004). Int. J. Mod. Phys. E 13, 1035.

[8] H. Arenhoevel, A. Fix, and M. Schwamb, Phys. Rev. Lett. 93, 202301 (2004); H. Arenhoevel, A. Fix, and M. Schwamb, in Proceedings of the 3rd International Symposium on the Gerasimov-Drell-Hearn Sum Rule and its Extensions (GDH 2004), Norfolk, Virginia, June 1-5, (2004), eds. S. Kuhn and J.-P. Cheng, World Scientific (2005), pp. 294, arXiv:nucl-th/0409015; M. Schwamb, (2006). Eur. Phys. J. A 28, Suppl. 1, 39.

[9] M. Tammam, A. Fix, and H. Arenhoevel, Phys. Rev. C 74, 044001 (2006); A. Fix, H. Arenhoevel, and M. Tammam, arXiv:nucl-th/0904.3840.

[10] H. Arenhoevel and A. Fix, Phys. Rev. C 72, 064004 (2005); A. Fix and H. Arenhoevel, Phys. Rev. C 72, 064005.

[11] V. Lensky, V. Baru, J. Haidenbauer, C. Hanhart, A. Kudryavtsev, and U.-G. Meissner (2005). Eur. Phys. J. A 26, 107.

[12] M.I. Levchuk, A.Yu. Loginov, A.A. Sidorov, V.N. Stibunov, and M. Schumacher (2006). Phys. Rev. C 74, 014004.

[13] GDH and A2@MAMI Collaborations, 23rd Students' Workshop on Electromagnetic Interactions, Bosen (Saar), Sept. 3-8, (2006).

[14] E.M. Darwish, in Proceedings of the 2nd Cairo International Conference on High Energy Physics (CICHEP II), German University in Cairo (GUC), Cairo, Egypt, January 14-17, (2006), edited by S. Khalil, AIP Conference Proceedings 881 (2007) 255.

[15] J. Ahrens et al. (2009). Phys. Lett. B 672, 328.

[16] V. Bernard, N. Kaiser, and U.-G. Meissner, Z. Phys. C 70, 483 (1996); A. Schmidt et al., Phys. Rev. Lett. 87, 232501 (2001); A. Schmidt, PhD dissertation, J. Gutenberg-Universitaet, Mainz, Germany (2001).

[17] S.B. Gerasimov, Sov. J. Nucl. Phys. 2, 430 (1966) [Yad. Fiz. 2, 598 (1965)]; S.D. Drell and A.C. Hearn, Phys. Rev. Lett. 16, 908 (1966).

[18] D. Drechsel, O. Hanstein, S. Kamalov, and L. Tiator, Nucl. Phys. A 645, 145 (1999); Phys. Rev. D 63, 114010 (2001); MAID Program, http://www.kph.uni-mainz.de/MAID/.

[19] R. Arndt, W. Briscoe, I. Strakovsky, and R. Workman, Phys. Rev. C 66, 055213 (2002), SAID database, http://gwdac.phys.gwu.edu.

[20] T. Sato and T.-S. H. Lee (1996). Phys. Rev. C 54, 2660.

[21] C. Fernandez-Ramirez, E. Moya de Guerra, and J.M. Udias, Ann. Phys. (N.Y.) 321, 1408 (2006); C. Fernandez-Ramirez, E. Moya de Guerra, and J.M. Udias (2008) Phys. Lett. B 660, 188.

[22] C. Fernandez-Ramirez, E. Moya de Guerra, and J.M. Udias (2006). Phys. Rev. C 73, 042201(R); (2007). Eur. Phys. J. A 31, 572.

[23] G. Blanpied et al., Phys. Rev. C 54, 025203 (2001); J. Ahrens et al., Eur. Phys. J. A 21, 323 (2004); S. Stave et al., (2006). Eur. Phys. J. A 30, 471.

[24] W.-M. Yao et al. (2006) J. Phys. G 33, .

[25] C. Alexandrou Ph. de Forcrand, H. Neff, J.W. Negele, W. Schroers, and A. Tsapalis (2005). Phys. Rev. Lett. 94, 021601 .

[26] C. Fernandez-Ramirez, E. Moya de Guerra, and J.M. Udias (2007). Phys. Lett. B 651, 369.

[27] D.G. Ireland, S. Janssen, and J. Ryckebusch, Nucl. Phys. A 740, 147 (2004); C. Fernandez-Ramirez, E. Moya de Guerra, A. Udias, and J.M. Udias, (2008). Phys. Rev. C 77, 065212.

[28] J. Haidenbauer and W. Plessas, Phys. Rev. C 30, 1822 (1984); J. Haidenbauer and W. Plessas, (1985). Phys. Rev. C 32, 1424.

[29] R. Vinh Mau, in Mesons in Nuclei I, edited by R.D. Wilkinson et al., (Plenum, London, 1979).

[30] H. Zankel, W. Plessas, and J. Haidenbauer, Phys. Rev. C 28, 538 (1983); H. Zankel and W. Plessas, Z. (1984). Phys. A 317, 45.

[31] E.M. Darwish (2002). PhD dissertation, J. Gutenberg University, Mainz, Germany, arXiv:nucl-th/0303056.

[32] S. Nozawa, B. Blankleider, and T.-S.H. Lee (1990). Nucl. Phys. A 513, 459.
[33] J.D. Bjorken and S.D. Drell (1964). Relativistic Quantum Mechanics (McGraw-Hill, New York,.
[34] M. Lacombe, B. Loiseau, J. M. Richard, R. Vinh Mau, J. Cote, P. Pires, and R. de Tourreil (1980). Phys. Rev. C 21, 861.
[35] B. Krusche, J. Ahrens, R. Beck, M. Fuchs, S.J. Hall, F. Haerter, J.D. Kellie, V. Metag, M. Roebig-Landau, and H. Stroeher(1999). Eur. Phys. J. A 6, 309.
[36] P. Benz et al. (1973). Nucl. Phys. B 65, 158.
[37] G. Chiefari, E. Drago, M. Napolitano, and C. Sciacca (1975). Lett. Nuovo Cim. 13, 129.
[38] M.A. Quraan et al. (1998). Phys. Rev. C 57, 2118.
[39] LEGS@BNL Collaboration, A.M. Sandorfi et al., http://www.legs.bnl.gov/; A.M. Sandorfi, private communication.